THE DYNAMICS OF MOLECULAR MATERIAL WITHIN 15 PCS OF THE GALACTIC CENTER

ALISON L. COIL
Astronomy Department
University of California at Berkeley
Berkeley, CA 94720
e-mail: acoil@astro.berkeley.edu
PAUL T.P. Ho
Harvard-Smithsonian Center for Astrophysics
60 Garden St. MS-78
Cambridge, MA 02138
e-mail: pho@cfa.harvard.edu

To appear in The Astrophysical Journal

ABSTRACT

We report the results of a 5-field mosaic of the central 15pc of the Galaxy in the (1,1) and (2,2) lines of NH₃. Two narrow filaments or streamers are seen running parallel to the Galactic plane. The southern streamer appears to carry gas directly toward the nuclear region from the 20 km sec⁻¹cloud. The eastern streamer, which we will denote the molecular ridge, appears to be the denser part of the 50 km sec⁻¹cloud which lies immediately east of the Sgr A East complex and extends in the south towards the 20 km sec⁻¹cloud. This ridge of gas carries the kinematical signatures of interactions with Sgr A East as well as a SNR which lies south of the Galactic center. The bulk motion of the gas, the enhanced line widths, and the heating of the molecular material all suggest an active evolutionary phase for the gas immediately adjacent to the nucleus.

Subject headings: Galaxy: center — ISM: clouds — ISM: molecules

1. INTRODUCTION

The two giant molecular clouds (GMCs) found within a few arcminutes of Sgr A* are known to be physically located at the Galactic Center and are seen interacting with the nuclear region. As discussed in Coil & Ho (1999, Paper 1), the 20 km \sec^{-1} cloud ("M-0.13-0.08"), lying 10 pc directly south of Sgr A* in projection (using $R_{\odot} = 8.5$ pc), appears to be feeding the circumnuclear disk (CND) via a molecular gas streamer called the "southern streamer" in Paper 1. The velocity gradient seen along the southern streamer places the 20 km sec⁻¹cloud slightly in front of the CND along our line of sight. The 20 km sec⁻¹cloud is connected to the other nearby GMC, the 50 km sec⁻¹cloud ("M-0.02-0.07"), by a ridge of gas and dust (Ho et al. 1991; Dent et al. 1993). This ridge appears to be compressed gas which wraps around Sgr A East and continues to the core of the 50 km sec⁻¹cloud, located ~ 2 ' (5 pc) east of Sgr A*. Sgr A East is an expanding shell of synchrotron emission which lies behind Sgr A* and the CND (Pedlar et al. 1989; Yusef-Zadeh et al. 1986). It is roughly 10 pc across and appears to be the result of an explosion which had an estimated total energy of $\sim 5 \cdot 10^{42}$ ergs (Mezger et al. 1989; Genzel et al. 1990), over an order of magnitude greater than the energy released by a typical SNR. It is unclear at present whether Sgr A East resulted from a highly energetic SNR, a typical SNR which expanded into a pre-existing bubble, or from a nuclear event peculiar to its location in the Galactic Center. It has been suggested that the tidal disruption of a star by the massive black hole Sgr A* could account for the energy and morphology of Sgr A East (Khokhlov & Melia 1996).

Sgr A East is expanding into the 50 km sec⁻¹ cloud

(Genzel et al. 1990; Ho et al. 1991; Serabyn, Lacy & Achtermann 1992), sweeping up gas in the western edge of the cloud, pushing it away from the nuclear region and creating a sharp, narrow ridge of dense gas. Kinematics of the ridge indicate that the gas in the 50 km sec⁻¹cloud is being pushed both to the east and behind Sgr A East along the line of sight, which would place the 50 km sec⁻¹cloud adjacent to and partially behind Sgr A East. The velocity shift resulting from this expansion is reported as 20 km sec^{-1} by Ho et al. (1991), as seen in north-south position-velocity diagrams taken along the western edge of the molecular ridge with a spectral resolution of 9.8 km sec^{-1} . Genzel et al. (1990) detect a shift of roughly 40 km $\sec^{-1}(\text{resolution} \sim 2.5 \text{ km sec}^{-1})$ in an east-west positionvelocity diagram taken +40" in declination relative to Sgr A^* , and Serabyn et al. (1992) (resolution 0.6 km sec⁻¹) also measure a shift of 40 km sec⁻¹based on spectra located just west of the ridge. The line width in the core of the 50 km \sec^{-1} cloud is FWHM=40 km \sec^{-1} , which is unusually broad for molecular cloud cores. The ridge of shocked gas is long and narrow, roughly 3 pc across and extending well over 10 pc north to south. Along the length of the entire ridge connecting the 20 km \sec^{-1} cloud with the 50 km sec⁻¹cloud and along the compression wave front there is a roughly north-south velocity gradient of $5-6 \text{ km sec}^{-1} \text{arcmin}^{-1}$.

Four HII regions are seen along the eastern edge of Sgr A East, in the vicinity of the dense ridge of gas at the edge of the $50~\rm km~sec^{-1}$ cloud. The HII regions all have velocities of $43\text{-}51~\rm km~sec^{-1}(Goss~et~al.~1985;$ Serabyn et al. 1992), and many have shell-like morphologies. The HII regions seem to be located in the $50~\rm km~sec^{-1}$ cloud, close

to the near edge along the line of sight. An H₂0 maser lies near the HII regions, possibly resulting from the expansion of Sgr A East into the surrounding molecular gas (Yusef-Zadeh & Mehringer 1995). Several 1720 MHz OH masers are detected around the Sgr A East shell, both along the southern rim and on the northwestern side near the CND (Yusef-Zadeh et al. 1996; Yusef-Zadeh et al. 1999). The 1720 MHz OH maser line has been found to be a good diagnostic of shock excitation, being found consistently at shock boundaries of supernova remnants (SNRs) (Frail et al. 1996). Yusef-Zadeh et al. (1996) propose that the group of masers on the southern rim traced the expansion of Sgr A East into the 50 km sec⁻¹cloud.

Figure 1 schematically outlines the relevant large-scale features in the central 15 pc of the Galaxy. Paper 1 discussed the southern streamer and its interactions with the CND. In this paper we report on $\mathrm{NH_3}(1,1)$ and (2,2) observations of the 50 km $\mathrm{sec}^{-1}\mathrm{cloud}$ and molecular ridge and discuss a SNR to the south of Sgr A East. Section 2 details the observations and data reduction, while Section 3 presents our results, which are discussed in Section 4. We present our conclusions in Section 5.

2. OBSERVATIONS AND DATA REDUCTION

We observed the metastable (J,K)=(1,1) and (2,2) transitions of NH₃ at the frequencies 23.694495 and 23.722633 GHz using the VLA, operated by NRAO, in DnC configuration. A total of five overlapping 2' fields were mapped towards Sgr A* on the night of 1995 Februarv 10. The mosaiced field of view is ~ 4 ' by 5', covering the inner 10-12 pc of the Galaxy. Results from the western three fields are presented in an earlier paper (Paper 1), and here we will show velocity-integrated images from all five fields but will focus mainly on the eastern two fields, which cover the western edge of the 50 km \sec^{-1} cloud and the molecular ridge. Our total bandwidth is 12 MHz centered at $v_{LSR} = 31.14 \text{ km s}^{-1}$ for the eastern two fields. The spectral resolution is 4.9 km sec⁻¹, corresponding to a total velocity coverage of 140 km sec⁻¹for our final 28 channels. We tapered our images to a synthesized beam size of $\sim 14'' \times 9''$ with a position angle of 12.6°. Details of the flux, phase and bandpass calibrations are described in Paper 1. Data from all five fields were jointly imaged and deconvolved in MIRIAD, effectively mosaicing the data in the u,v plane. We employed the same CLEANing technique as in Paper 1, where we added a flat offset of zero-spacing flux during the CLEAN process which was removed after CLEANing. The images presented in this paper have all been corrected for the primary beam response unlike many of the images shown in Paper 1 which were tapered at the edges, resulting in a lower correction (and lower noise) at the edges of those images. All coordinates are B1950 epoch.

3. RESULTS

3.1. Velocity-Integrated Emission

Figure 2 is an NH₃ velocity-integrated mosaic map of all five fields seen in contours overlaid on a color 20 cm continuum image of Sgr A East and West (Lang, Morris, & Echevarria 1999). Sgr A West is the oversaturated black region, inside of which the mini-spiral of ionized gas streamers converge near the location of Sgr A*. The red emission traces Sgr A East, which is offset from Sgr A West. The contours display $NH_3(1,1)$ emission on the left and $NH_3(2,2)$ on the right. There are two prominent north-south streamers in these images. The "southern streamer" (see Paper 1) connects the circumnuclear disk (CND) surrounding the ionized gas mini-spiral with the 20 km sec⁻¹ to the south. The northern half of the 20 km sec^{-1} cloud is shown in these images, located at R.A.= $17^{h}42^{m}28^{s}.5$, Dec.= $-29^{\circ}02'.0$. As reported in Paper 1, we find a velocity gradient of $\sim 5-8$ km sec⁻¹arcmin⁻¹ along the southern streamer with the gas redshifting to the north, which places the 20 km sec⁻¹cloud in front of the nuclear region along the line of sight. Details of this streamer are discussed further in Paper 1.

The other long streamer in Figure 2 is the molecular ridge which traces the denser parts of the 50 km sec⁻¹cloud, including the core of the cloud and gas in the southern part of the GMC where Sgr A East is expanding into the cloud. There is strong emission in the northern half of the streamer where the ridge wraps around the eastern edge of Sgr A East. The $50~\mathrm{km~sec^{-1}}$ cloud continues to the east and north beyond the edge of the figure (Zvlka, Mezger, & Wink 1990; Serabyn et al. 1992; Dent et al. 1993). The narrow, concentrated ridge of molecular gas wraps around Sgr A East and continues to the south at a lower flux level, past -29°03′ to the edge of our sampled field. The width of the molecular ridge is roughly constant along its length, though to the south of Sgr A East the emission is fluffier and more spread out. The gas is highly clumped, and the sharp edges where the intensity of the emission increases quickly are not smooth along the length of the ridge. The emission in the northern part of the ridge falls off more steeply at the edges than in the southern part, which may indicate that the gas to the north is more confined than to the south. The northern part of the ridge closely follows the arc of Sgr A East, appearing to wrap around the expanding shell. There are many small bumps and protrusions of the gas which are seen in both the $NH_3(1,1)$ and $NH_3(2,2)$ data, including the location of the peak emission in the northern part of the ridge. The flux in the ridge is higher in the north, and the peak is found lying along the easternmost part of Sgr A East.

There is an extension of the gas projected onto Sgr A East near Dec.=-28°59′0.5″, where there is a large hollow bubble in the continuum emission greater than 1′ in size, clearing gas into the molecular ridge to the east and Sgr A West and the CND to the west. This hollow bubble can be seen clearly in Figure 2 where there is a yellow hollow region inside the red emission from Sgr A East, near the southeastern edge of Sgr A East in between the two streamers. The molecular emission closely traces the eastern and western edges of the bubble, wrapping just

around the outside of the hollow area. Morphologically it appears that the bubble is interacting with both the molecular ridge and the gas in the northern part of the streamer connecting the 20 km \sec^{-1} cloud to the CND (the "southern streamer" in Paper 1). To the south of this bubble, there is another region where the gas from the ridge has a protrusion to the west, near the southern edge of Sgr A East. At this location a connection has been imaged between the molecular ridge and the 20 km \sec^{-1} cloud in NH₃(3,3) (Ho et al. 1991). We do not image a connection here, but connections between these features have also been imaged in 13 CO(2-1) (Zylka et al. 1990) and submillimeter thermal dust emission (Dent et al. 1993 and Zylka 1997).

Along the eastern edge of Sgr A East, the molecular ridge continues without break or bend to the south past where the continuum emission stops. The separation between the two streamers in the southern half of these images is roughly constant, which may in part be affected by the deep negative sidelobes due to the lack of short spacings and the fact that the mapped region is sampled only at full-beam spacings. However, the narrowness of the ridge in the southeast is not likely due to the primary beam response as our primary beam includes much of the empty region in the southeast as seen in Figure 3. This image shows our effective mosaiced primary beam pattern on the sky and labels the percentage level of flux sampling over the region. We have not plotted emission with a gain below 15% as those features are unreliable. While the beam response is not uniform across the field, it is at least 50% everywhere, so that at most our flux may be down by a factor of two in the very central region. The northernmost part of the molecular ridge shows high flux near the edge of the primary beam, indicating that the ridge continues to the north beyond our sampled field. Our limited velocity range may also cause undersampling in this region. An area which is interesting for its lack of flux is the lower left of the map, to the east of the southern part of the molecular ridge, where with a 100% beam response level we do not detect emission.

Many of the most striking features seen in Figure 2 are apparent in both $\mathrm{NH_3}(1,1)$ and $\mathrm{NH_3}(2,2)$ emission. Similarities between the images include the narrow width of the molecular ridge, the location of the peak emission in the ridge, and the extension of gas into Sgr A East at the eastern side of the bubble. The localized emission in between the two streamers at the southern edge of Sgr A East (Dec.=-29°00′30″) is seen in both maps, and the structure of the 20 km sec⁻¹cloud is very similar in the $\mathrm{NH_3}(1,1)$ and $\mathrm{NH_3}(2,2)$ images, where the many peaks and fingers of emission are the same. The main differences between the $\mathrm{NH_3}(1,1)$ and $\mathrm{NH_3}(2,2)$ velocity-integrated emission maps are seen concentrated near the nuclear region (discussed at length in Paper 1).

Figure 4 shows the same continuum image as Figure 2 with our velocity-integrated NH₃ contours, but here the stretch of the grey-scale has been altered to bring out lower level features in the 20 cm continuum image. Four small HII regions are located just off the eastern edge of Sgr A East, seen here as small black spots at the top

left of the continuum image (Ekers et al. 1983: Goss et al. 1985). The molecular ridge of gas is narrowly confined to the region in between the eastern edge of Sgr A East and the HII regions 0.5' away. In the $NH_3(2,2)$ image the northernmost part of the streamer above Dec.=-28°58′30″ is narrower and is seen just at the edge of Sgr A East and does not extend eastward to the northern two HII regions. The southernmost HII region, located at R.A.= $17^{h}42^{m}41^{s}$, Dec.= $-28^{\circ}59'12''$ and labeled D in discussions of this HII region grouping (Goss et al. 1985), appears to be still embedded in dense molecular gas where the contours peak sharply into a small clump on the eastern edge of the ridge. This HII region is the only one of the four which does not have a shell-like morphology, which could indicate that it is in an earlier stage of development. It may either be younger than the other HII regions or its expansion or flow out of the cloud may have been slowed by the dense gas surrounding it.

In Figure 4 there is an intriguing association between the continuum and molecular line emission along the 20 km sec⁻¹cloud in the southwestern part of the image. The $20~\rm km~sec^{-1} cloud$ follows the arc of the two dark streaks of continuum emission known as Sgr A-F and Sgr A-E (the 'wisp') (Ho et al. 1985; Yusef-Zadeh & Morris 1987). Ho et al. (1985) suggest that these two non-thermal arcs trace the edge of a SNR which may be expanding into the 20 km sec⁻¹cloud, compressing the gas in the GMC. Figure 4 reveals a hollow shell extending across the southern half of the image, including these arcs to the southwest and continuing up around the southern edge of Sgr A East and extending out along another curved arc centered at R.A.= $17^{h}42^{m}40^{s}$, Dec.= $-29^{\circ}00'30''$. The southern edge of Sgr A East has a curved shape seen in Figures 2 and 4 which follows the arc of the SNR, opposing the curvature of the roughly spherical Sgr A East shell itself.

In the $NH_3(3,3)$ velocity-integrated map (Ho et al. 1991, see Figure 1) the molecular ridge does not continue as far to the south as it does in the $NH_3(1,1)$ and $NH_3(2,2)$ maps. The $NH_3(3,3)$ image shows the ridge following the eastern arc of Sgr A East down to Dec.=-29°00′30″ where the ridge then splits off from Sgr A East and continues to the southwest towards the 20 km sec⁻¹cloud. The ridge does not continue south of Dec.= $-29^{\circ}02'$. In the NH₃(1,1) and $NH_3(2,2)$ images, the ridge has the same behavior as the NH₃(3,3) emission down to Dec.=-29°02', where instead of connecting with the 20 km sec⁻¹cloud as in the $NH_3(3,3)$ image, it continues further south to Dec.=-29°03′. Because the length of the southern part of the ridge is different from the $NH_3(3,3)$ image, we investigate this emission further to look for possible contamination by sidelobes from the 20 km sec^{-1} cloud. Figure 5 displays velocity-integrated maps of the southern two fields of the NH₃(1,1) data imaged individually without any mosaicing of other fields. The image on the left is from the southeastern field only and does not show any emission from the 20 km sec⁻¹cloud. The southern part of the ridge can not be due to sidelobe structure from the 20 km sec⁻¹cloud as the ridge is seen clearly in the primary beam centered on this region. The southwestern field is shown on the right, where the 20 km sec⁻¹cloud and part of the southern streamer is seen. The negative contours are due to sidelobe structure, as are the positive contours in the eastern half of the image. This figure shows that the southern half of the ridge is not strongly affected by sidelobe structure from the 20 km $\rm sec^{-1}cloud$. We also show position-velocity cuts taken along the southern part of the ridge and the 20 km $\rm sec^{-1}cloud$ in Figure 6 to see if the kinematics of the gas in the ridge and the GMC are identical, as would result from strong sidelobe contamination. The position-velocity diagrams from cut A do not match those from cut B in either $\rm NH_3(1,1)$ or $\rm NH_3(2,2)$ emission. The locations of the velocity peaks, as well as the line widths, do not correlate between the two cuts. We conclude that the structure of the southern part of the ridge is real and that contamination by sidelobes from the $\rm 20~km~sec^{-1}cloud$ is not important.

3.2. Comparison with 1.3mm Dust Emission

Figure 7 overlays contours of 1.3mm emission (Zylka 1997) in the Sgr A complex with a grey-scale image of our $NH_3(1,1)$ velocity-integrated emission. The 1.3mm map traces both free-free emission from ionized gas in the Sgr A West HII region and thermal dust emission from the GMCs which traces the total column of gas. The 1.3mm data has an angular resolution of 11" and is quite comparable to the resolution of the NH₃ data. As single dish data however, the 1.3mm image is more sensitive to emission on larger scales than our interferometric data, which are missing the shortest spacing information, so that the 1.3mm map better traces the large-scale structure of the material in the region. The peak of the 1.3mm emission delineates the ionized gas in the Sgr A West HII region where the southern half of the inner edge of the CND can be seen in grey-scale at the lower edge of the spiral. The streamer to the south which connects the nuclear region with the 20 km sec⁻¹cloud is present in both the dust and molecular gas images, where the 1.3mm contours closely trace the $NH_3(1,1)$ emission. The core of the 20 km sec⁻¹cloud is seen at the lower edge of the 1.3mm image, beyond the spatial coverage of our $NH_3(1,1)$ map. The dark grey-scale emission traces only the northern part of the 20 km \sec^{-1} cloud, where the GMC is becoming narrower and elongated, connecting with the nuclear region. There is extremely excellent agreement in detailed spatial structures between the $NH_3(1,1)$, $NH_3(2,2)$, and dust maps. The other dark region of the grey-scale $\mathrm{NH_3}(1,1)$ map marks the core of the 50 km sec^{-1} cloud in the upper left of the image, near RA= $17^h42^m40^s$ and Dec.= $-28^{\circ}59'$. The entire 50 km sec⁻¹GMC includes fluffier emission not traced by the NH₃ emission in the molecular ridge, and extends to the north beyond the extent of our images. Near the 50 km sec⁻¹cloud core and towards the south where the 50 km sec^{-1} cloud bends towards the Sgr A West spiral, the $NH_3(1,1)$ emission in the molecular ridge closely corresponds to the areas of highest dust column density as seen in the 1.3mm image. However, at the cloud core the $NH_3(1,1)$ emission does not continue to the eastern edge of our field where the dust column density is still high.

It has been suggested that the 50 km sec⁻¹cloud may also feed the CND via a streamer of gas and dust in a similar manner as the 20 km sec⁻¹cloud. An intriguing gas streamer has been seen in single-dish HCN emission

by Ho (1994), where a distinct narrow streamer appears to connect the western edge of the 50 km sec^{-1} cloud with the nuclear region. This streamer is seen well in the individual channel maps, specifically around 60 km sec^{-1} . A similar streamer connecting the 50 km sec^{-1} cloud with the CND has been imaged in ¹³CO(2-1) emission by Zylka et al. (1990). The streamer can be seen in the channel map showing emission from 50 km sec⁻¹to 60 km sec⁻¹(their Figure 5.d). This streamer has not been seen in other millimeter and sub-millimeter observations (Mezger et al. 1989; Dent et al. 1993) nor in interferometric NH₃(3,3) data (Ho et al. 1991), nor do we detect it here. It remains unclear whether the 50 km sec⁻¹cloud directly feeds the nuclear region or whether the streamer is being projected along the line of sight, though it is clear from the dust maps that if an eastern streamer exists it must have a lower column density than the southern streamer. There is also an intriguing finger of dust emission to the north of the 50 km sec⁻¹cloud which points in towards the nucleus, at the top of the CND near RA= $17^{h}42^{m}33^{s}$ and Dec.= $-29^{\circ}58'$.

The $NH_3(1,1)$ molecular ridge continues to the south of the 50 km sec⁻¹cloud core where the dust emission is lower (Dec.= $-29^{\circ}00'$ to $-29^{\circ}03'$). The ratio of flux in the 50 km sec⁻¹cloud and the 20 km sec⁻¹cloud to the southern part of the ridge is higher in $NH_3(1,1)$ than in 1.3mm dust emission. This implies that the relative prominence of the $NH_3(1,1)$ emission in the southern part of the ridge as compared to the 1.3mm emission is due in part to the contouring of the 1.3mm image and is most likely due to the sensitivity of the 1.3mm map to extended lower density material. The long molecular ridge as seen in the $NH_3(1,1)$ image has a constant, narrow width which is reflected in the dust emission only along the northern half of the streamer. At the southern tip of the molecular ridge there is a U-shaped feature in the 1.3mm image connecting the ridge with the eastern side of the 20 km sec⁻¹cloud. A connection between the two GMCs has been imaged in $NH_3(3,3)$ (Ho et al. 1991), with similar coverage as our $NH_3(1,1)$ and $NH_3(2,2)$ maps, and in submillimeter continuum (Dent et al. 1993), which has similar coverage as the 1.3mm emission shown here. It appears from Figure 7 that the two GMCs are not entirely separate entities connected only by a thin ridge of gas, but the clouds and ridge may be intimately connected and part of a coherent larger structure of gas lying along the Galactic plane.

Striking features of our velocity-integrated $\mathrm{NH}_3(1,1)$ and $\mathrm{NH}_3(2,2)$ images include the narrowness of the two streamers seen lying along the Galactic plane and the roughly constant separation between them. Our lack of zero-spacing information prevents us from concluding whether the narrowness of the streamers is meaningful. The roughly constant spacing between the two streamers in our maps is not seen in other images of the region and may be due to the negative trenches resulting from side-lobe structure in between the two streamers (see Figure 2). Comparing our maps to the $\mathrm{NH}_3(3,3)$ and $1.3\mathrm{mm}$ emission it seems that we are missing structure in between the two streamers at the southern edge of Sgr A East. The total column density as seen by the dust emission shows the molecular ridge curving around Sgr A East in

the south, pointing towards the southern streamer as it approaches the nuclear region. The $\mathrm{NH_3}(3,3)$ map more closely follows the dust emission in this region than our $\mathrm{NH_3}(1,1)$ and $\mathrm{NH_3}(2,2)$ images, and in the $\mathrm{NH_3}(3,3)$ image there are two connections seen between the streamers: one along the southern edge of Sgr A East, which is also seen in the dust emission, and another connection further south at Dec.=-29°02′. Our images do not show either of these connections, which may be a result of the negative sidelobe trench or may also be a temperature effect. The 1.3mm dust emission does show low-level flux along the southern part of the molecular ridge but it is not confined to a narrow streamer, whereas the northern half of the ridge is narrow in both our maps and the 1.3mm map.

3.3. $NH_3(2,2)/NH_3(1,1)$ Line Ratio Map

Figure 8 indicates regions of heating as derived from the $NH_3(2,2)/NH_3(1,1)$ line ratio where the dark regions trace heated gas. The rotation temperature of the gas can be derived from the ratio of $NH_3(2,2)$ to $NH_3(1,1)$ observed brightness temperatures if the lines are optically thin. In the optically thin limit a $NH_3(2,2)/NH_3(1,1)$ ratio of 0.5 implies a rotation temperature of 21 K, a ratio of 1 corresponds to 33 K, a ratio of 1.5 corresponds to 49 K, and a ratio of 2 corresponds to a rotation temperature of 73 K. These values are in actuality a lower limit on the rotation temperature, because if line opacities are substantial a correction must be made based on the optical depth of the NH₃(1,1) line (see Figure 4 of Ho & Townes 1983 for details of how the rotation temperature depends on the optical depth). Nevertheless, a simple map of the $NH_3(2,2)/NH_3(1,1)$ line ratio can still provide heating information if the optical depth of the gas does not change significantly over the region. The contours in Figure 8 are from the 6 cm continuum map of Sgr A East as seen in Figure 2, overlaid on a grey-scale map of the velocity-integrated $NH_3(2,2)/NH_3(1,1)$ ratio, with the dark regions of high $NH_3(2,2)/NH_3(1,1)$ ratio showing hotter gas. Heating in the nuclear region, near the CND, was discussed in Paper 1. Here we focus on the molecular ridge and the 20 km sec⁻¹cloud, where most of the heating is along the western edges of these features. There is not much heating seen along the northern part of the inner edge of the molecular ridge where the gas appears to be directly interacting with Sgr A East. We are unable to estimate optical depths at this location from our spectra and can not determine whether this apparent lack of heating is real. The extension of gas projected onto Sgr A East shows signs of heating, as does the small region of emission seen in between the two streamers at the southern edge of Sgr A East. The southern part of the molecular ridge shows heating on both the eastern and western sides, much like the 20 km sec^{-1} cloud emission. Much of the heating in this map is along the edges of the streamers. This is not an imaging artifact, where the edges are darker due to cutoffs in the processing of the maps, as $NH_3(2,2)/NH_3(1,1)$ ratio maps made with many different cutoffs show all of the same regions of heating. The apparent edge heating may well be affected by optical depth differences along the edges of the streamers.

3.4. Velocity Centroid and Dispersion Maps

Figures 9 and 10 display kinematic features of the gas in the molecular ridge as well as the southern streamer. Figure 9 maps the mean velocity of the gas at each pixel, where the dark regions correspond to higher velocity gas. The grey-scale ranges from 15 km sec⁻¹ for the white areas to 60 km sec⁻¹in the black regions. There is an overall velocity gradient along the length of the molecular ridge, where the gas in the northern half of the ridge has been redshifted by $\sim 20 \text{ km sec}^{-1}$. The mean velocity does not appear to increase linearly along the length of the streamer, but instead the northern half of the streamer appears to be at $\sim 40 \text{ km sec}^{-1}$ where the ridge wraps around the edge of Sgr A East, while the southern part of the streamer also appears to be at $\sim 20 \text{ km sec}^{-1}$. This change in velocity near the southern edge of Sgr A East, where the ridge does not appear to be directly interacting with Sgr A East, can be seen in both the $NH_3(1,1)$ and $NH_3(2,2)$ maps. There are also noticeable smaller dark regions of pronounced redshifting of the gas. This occurs at the inner edge of the molecular ridge where the gas appears to extend into Sgr A East in projection. This gas is also heated, as seen in Figure 8, and may be located at the far side of Sgr A East, being redshifted along the line of sight by the expansion of Sgr A East. The redshifting of the extension is seen to a lesser degree in the $NH_3(2,2)$ image, where the gas is highly redshifted at the base of the extension but the mean velocity decreases further along the extension. There is another intriguing localized region of redshifting seen in the $NH_3(1,1)$ image at the outer edge of the molecular cloud, near Dec.=-29°00′45″. The eastern edge of the 20 km sec⁻¹cloud is also redshifted relative to the rest of the cloud, and at the lower tip of the cloud there is a small area of redshifted gas where there are a few contours from the 6 cm continuum map. This non-thermal feature, dubbed the "wisp" (Ho et al. 1985), has been proposed to be the result of a supernova remnant interacting with the ambient molecular gas. The redshifting of the molecular gas in the 20 km sec⁻¹cloud at this location as seen in Figure 9 may be explained by this idea.

Figure 10 spatially maps the velocity dispersion of the molecular gas in grey-scale, where darker regions indicate gas with higher dispersion. The darkest regions around Sgr A West are where the gas from the southern streamer is accreting onto the CND (Paper 1). The southern tip of the 20 km sec⁻¹cloud shows high velocity dispersion at the "wisp," which further strengthens the claim that the "wisp" is the result of a SNR (Ho et al. 1985). Along the western molecular ridge, there is little change in dispersion in the $NH_3(1,1)$ image across the northern half of the ridge from east to west where the ridge wraps around the eastern side of Sgr A East, possibly indicating that all of this gas has been processed and is in a post-shock phase, which is consistent with the lack of heating here (see Figure 8). In the $NH_3(1,1)$ image there are two small darker spots of higher dispersion along the northeastern edge of the ridge which may be the result of infall or outflows from the HII regions seen in contours. The $NH_3(2,2)$ image shows some line broadening along the inner edge of the northern part of the ridge facing Sgr A East, where the gas is darker along the western side of the ridge. As in the velocity centroid map (Figure 9) there is a demarcation between the upper and lower halves of the molecular ridge, where wide variations in dispersion are seen throughout the southern half of the ridge. In particular, there are concentrated regions of increased velocity dispersion along the inner, western edge of the ridge which are not seen in the northern half. The gas in the lower part of the ridge generally appears to be more perturbed than the gas directly adjacent to Sgr A East. Many of the dark regions in the $NH_3(2,2)$ map also show unusual mean velocities in Figure 9 and are heated as seen in Figure 8. Clearly the gas along the lower inner edge of the molecular ridge is highly perturbed. This is consistent with the SNR to the south of Sgr A East impacting the gas.

3.5. Position-Velocity Diagrams

We further investigate the kinematics of the gas using position-velocity diagrams in Figures 11 and 12. Figure 11 displays position-velocity information for $NH_3(1,1)$ and $NH_3(2,2)$ emission as well as the $NH_3(2,2)/NH_3(1,1)$ ratio along four cuts running the length of the molecular ridge. The datacubes have been smoothed in R.A. and Dec. to enhance the general spectral features and increase the signal-to-noise. The $NH_3(2,2)/NH_3(1,1)$ datacube has also been Hanning smoothed in velocity space. The diagrams for cut A from the outer side of the streamer, furthest from Sgr A East, show a velocity gradient along the southern part of the streamer starting at 20 km sec⁻¹at the southern tip of the streamer and increasing past 55 km sec⁻¹towards the middle of the streamer. The velocities then decrease again to the north at the location on the velocity-integrated map where the most emission is found. The overall gradient along the ridge traces out a backwards "C" shape in position-velocity space in the $NH_3(1,1)$ diagram. The $NH_3(1,1)$ diagram shows a large line width and blueshifted gas at the northern edge of the cut near the southernmost HII region in the continuum image (Figure 2). This blueshifted emission may be the result of outflows from this HII region. Further south along cut A at the location of the dark emission on the eastern edge of the ridge as seen in $NH_3(1,1)$ emission in Figure 9, there is an asymmetric lobe of redshifted emission extending from 30 km \sec^{-1} to 80 km \sec^{-1} in the NH₃(1,1) position-velocity diagram and from 40 km sec⁻¹to 70 km \sec^{-1} in the $NH_3(2,2)$ diagram. This gas is not only redshifted, but has a higher velocity dispersion than the gas towards the south as seen in both the $NH_3(1,1)$ and $NH_3(2,2)$ diagrams. This broader gas may be similar in nature to gas further north. (The $NH_3(1,1)$ gas should be slightly more spread out in velocity space due to an unresolved hyperfine line located 8 km sec⁻¹away from the main line, which causes some artificial line broadening. Our velocity resolution is able to resolve the hyperfine structure in the $NH_3(2,2)$ gas so that the $NH_3(2,2)$ diagrams do not show artificially broadened line widths. However, NH₃(1,1) emission with line widths across 50 km sec⁻¹can not entirely be due to hyperfine blending.) The $NH_3(2,2)/NH_3(1,1)$ diagram indicates heating, where dark regions trace hotter gas. This redshifted gas shows heating for the component at $35-40 \text{ km sec}^{-1}$, but not for the highly redshifted gas. An increase in line width is also seen at the southernmost tip of the streamer, where there is low-level emission extending from -10 km \sec^{-1} to 50 km \sec^{-1} and from 65 km \sec^{-1} to 85 km \sec^{-1} . This gas appears to be highly perturbed, and the NH₃(2,2)/NH₃(1,1) diagram shows that the component of this gas at high velocities is heated.

Cuts B and C, taken through the central part of the ridge, show a similar overall velocity gradient as cut A, though the gas does not trace out a backwards "C" pattern in position-velocity space as it does in cut A. The global velocity gradient is of order 7 km sec⁻¹arcmin⁻¹, in good agreement with the gradient found by Serabyn et al. (1992). In the $NH_3(1,1)$ diagrams there is some low-level high-velocity emission in the central region, at velocities of 70 km \sec^{-1} to ≥ 100 km \sec^{-1} . In the NH₃(2,2) diagrams there is redshifted gas which continues as a feature at 70-80 km sec⁻¹along the southern length of the ridge, extending in cut C to velocities $\geq 100 \text{ km sec}^{-1}$. The $NH_3(2,2)/NH_3(1,1)$ diagrams for B and C show that this highly redshifted gas at $\geq 70 \text{ km sec}^{-1}$ is heated. There is also heating in the low-velocity ($\leq 0 \text{ km sec}^{-1}$) gas at the southern end of the ridge, where the velocity dispersion increases. The $NH_3(1,1)$ position-velocity diagram for cut D, which is taken along the inner edge of the ridge, where the streamer is adjacent to Sgr A East, looks very similar to the $NH_3(1,1)$ diagram for cut A. The backwards "C" shape is again apparent in the northern half of the diagram, where the gas in the middle of the streamer has been redshifted to a central velocity of 60 km sec⁻¹as in cut A, whereas in cuts B and C the central velocity is 45 km \sec^{-1} . In the NH₃(2,2) diagram for cut D this part of the streamer is also highly redshifted, with a very pronounced kink at 50 arcsec on the y-axis. Gas in the southern part of cut D has a very large dispersion as seen in the other diagrams, covering our entire sampled velocity range from below -35 km sec⁻¹to greater than 100 km \sec^{-1} . There appears to be a hole in position-velocity space in the southern half of the diagrams from 0 arcsec to -75 arcsec on the y-axis and from 40 km sec^{-1} to 70 mkm \sec^{-1} on the x-axis. At the location of this hole the central velocity of the gas is at $\sim 30 \text{ km sec}^{-1}$ and has a narrow line width compared to the gas elsewhere along the streamer. The $NH_3(2,2)/NH_3(1,1)$ diagrams indicate that the gas at the edges of the hole is heated.

Position-velocity diagrams taken east to west across the molecular ridge are seen in Figure 12. We again show diagrams for both $NH_3(1,1)$ and $NH_3(2,2)$ emission, as well as the $NH_3(2,2)/NH_3(1,1)$ ratio to show the heated The $NH_3(1,1)$ emission for cuts A and B, taken across the northern section of the ridge, show a velocity gradient from low velocities along the eastern edge of the ridge to higher velocities along the western edge, facing Sgr A East. The gas in the east is seen at velocities as low as -5 km \sec^{-1} whereas in the west, ~ 3 pc away in projection, gas is seen at velocities up to 85 km sec^{-1} . The $NH_3(2,2)/NH_3(1,1)$ diagram for cut A shows that the redshifted gas to the west is heated, as seen from the dark region at 70 km \sec^{-1} . The NH₃(2,2) diagram for cut B, which intersects the region of the streamer which extends into Sgr A East in projection, shows an "O" shape of emission in position-velocity space. In the east the central velocity of the gas is 40 km sec⁻¹, whereas along the extension the gas is both red- and blueshifted by \sim 40 km sec⁻¹before it combines again at a central velocity of 35 km sec⁻¹. Both Genzel et al. (1990) and Serabyn et al. (1992) report a velocity shift of \sim 40 km sec⁻¹in the molecular ridge where it is interacting with Sgr A East. The NH₃(2,2)/NH₃(1,1) diagram shows that the gas in the west at 35 km sec⁻¹is strongly heated. This gas is being impacted by the expansion of either Sgr A East or the hollow bubble seen in Figure 2 into the ridge, causing red- and blueshifting of the gas. The redshifted emission has a higher flux level than the blueshifted emission, indicating that more of the gas is located behind Sgr A East than in front of it.

Cut C is taken in the middle of the ridge near the southern edge of Sgr A East where the ridge no longer wraps around Sgr A East but continues to the south. Here the gas in the ridge does not have the east to west redshifting velocity gradient, nor is the "O" shape apparent. The $NH_3(2,2)/NH_3(1,1)$ diagram shows that the gas is heated on the eastern and western edges of the ridge, and that in the center of the ridge the gas at high velocities $(\sim 75 \text{ km sec}^{-1})$ is also heated. Cuts D and E, taken from the southern part of the streamer, both indicate that the gas in the south has a higher velocity dispersion than the gas to the north. There is low-level emission at all velocities in our sampled velocity range, from ≤-35 km \sec^{-1} up to ≥ 100 km \sec^{-1} . The high-velocity gas (≥ 70 km \sec^{-1}) is heated as seen in the NH₃(2,2)/NH₃(1,1) diagrams. The very low-velocity gas (<-10 km sec⁻¹) is also heated, though to a lesser degree. In opposition to the redshifting velocity gradient seen in the northern part of the ridge, here in the south the gas blueshifts slightly towards the western edge of the streamer facing Sgr A East. The western edge of the streamer is heated as seen in cut E, with a central velocity of 20 km sec^{-1} .

3.6. Derived Physical Parameters

We estimate that we are recovering 20-25\% of the single dish $NH_3(1,1)$ flux in our interferometric data by comparing the peak observed brightness temperature in each streamer with the single-dish antenna temperatures (corrected for beam efficiency and atmospheric attenuation) at the same locations reported by Armstrong & Barrett (1985), after convolving our data to the 1.4' beam of the Haystack data. We are not sensitive to structures greater than 1' in extent, nor do we have short spacing information which would increase our total flux. We list derived physical parameters for the $NH_3(1,1)$ peak flux locations in the northern and southern parts of the ridge in Table 1. A mean optical depth was derived for each part of the ridge from spectra with clear hyperfine structure. A total of 8 and 10 spectra were used to determine the optical depth in the northern and southern parts of the ridge, respectively. To derive the physical parameters we used the equations outlined in Paper 1, section 3.6. An estimation of the rotation temperature requires the $NH_3(1,1)$ optical depth and the ratio of $NH_3(2,2)$ to $NH_3(1,1)$ brightness temperatures at that location. Masses for each part of the ridge are estimated from the derived column density, which depends on the optical depth and excitation temperature. These mass estimates for the dense component of the ridge are reasonable even though we are not imaging all of the flux as the missing flux corresponds to more extended structures and may include some of the 50 km \sec^{-1} cloud. We find a mass for the molecular ridge of 1.5 10^5 M_{\odot} , which agrees quite well with masses for the molecular ridge calculated by Zylka et al. (1990) and Serabyn et al. (1992).

4. DISCUSSION

4.1. Interaction Between Sgr A East and the 50 km $\,\,\mathrm{sec^{-1}Cloud}$

The northern part of the molecular ridge traces the densest parts of the 50 km sec⁻¹cloud, including the core and the ridge of dense gas being impacted by Sgr A East. The ridge may be processed and post-shock, as there is not a significant increase in density or temperature along the western edge of the ridge (see Figures 2 and 8) as one might expect if the inner edge was being more directly impacted by Sgr A East than the outer edge. There is also not a pronounced increase in velocity dispersion along the inner edge of the ridge in the $NH_3(1,1)$ emission, though in the $NH_3(2,2)$ data the velocity dispersion does increase somewhat along the inner edge (see Figure 10). If the ridge is processed and the shock wave has reached the far side of the ridge where the string of HII regions is, it is possible that the shock wave itself created the collapse which formed the HII regions. Yusef-Zadeh & Mehringer (1995) find an H₂O maser associated with one of the four sources in the HII region which could indicate that the shock from the expansion of Sgr A East has reached the HII regions.

There is an increase in the central velocity of the gas along the inner edge in the northern part of the ridge, as seen in the position-velocity diagrams for cuts A and B in Figure 12. The position-velocity diagram for the $NH_3(2,2)$ emission across the densest part of the ridge. near the southernmost HII region (cut B), shows both red- and blueshifting of the gas. More gas is redshifted than blueshifted, indicating that as the ridge wraps around the expanding shell, it is more behind Sgr A East than in front of it (evidence that at least part of the gas cloud lies in front of Sgr A East is also seen by Liszt et al. 1983). These diagrams include emission from the small gas extension which is projected onto Sgr A East. In the NH₃(1,1) diagram, this gas is redshifted to 55 km \sec^{-1} and 75 km \sec^{-1} , while in the NH₃(2,2) diagram an "O" shape is seen. This "O" shape would most naturally result from an expanding bubble. The gas around the edge of the bubble has no velocity shift along the line of sight, whereas gas in the middle of the bubble is being pushed both towards and away from the observer, creating redand blueshifted emission in the position-velocity diagram in the middle of the cut through the bubble. The spatial extent of the gas extension therefore defines the extent of the bubble. In the continuum image of Sgr A East the molecular gas extension lies just inside a larger bubble in the eastern region of Sgr A East. The bubble seen in the continuum image has a much larger physical extent than the bubble defined by the molecular gas extension.

It is unclear whether these two features are related and interacting with one another.

4.2. Southern SNR Interacting with the Molecular Ridge

The morphology and kinematics of the northern and southern parts of the molecular ridge suggest different histories along the length of the streamer. Figure 2 shows that the morphology of the southern part of the streamer is fluffier and less confined than the northern part. In the south there are more protrusions and clumps in the gas, and the flux level is lower than in the north. While Figure 8 indicates no clear temperature differences between the northern and southern parts, the velocity centroid image (Figure 9) shows that the entire southern half of the ridge is at a lower velocity than the northern half and that the transition between the two regions is not smooth. The velocity dispersion map (Figure 10) reveals that the northern half of the ridge has roughly the same dispersion throughout while the southern half has widely varying dispersions as well as regions of very high dispersion indicating perturbed gas. The position-velocity diagrams taken across the ridge (Figure 12) show a different gradient from east to west in the north and south. The diagrams taken across the northern part of the ridge show an east to west redshifting of the gas, while in the south the gradient blueshifts to the west.

The northern and southern parts of the ridge are spatially and kinematically connected but are clearly being acted upon by different forces. The entire ridge is one structure, but currently there are two distinct shells expanding into the northern and southern parts separately. Sgr A East is expanding into the 50 km sec⁻¹cloud, and the northern half of the molecular ridge traces this impact. There is apparently a SNR to the south of Sgr A East which is interacting with the southern half of the ridge as well as Sgr A East and the southern streamer. In terms of its galactic coordinates the SNR is "G 359.92" -0.09". Images of this SNR can be seen in Yusef-Zadeh and Morris (1987), in their Figures 2 and 3 of 20 cm continuum emission, which clearly show a circular feature south of Sgr A East. The SNR can also be seen in Pedlar et al. (1989), Figure 5b, another 20 cm continuum image of Sgr A East. This SNR is interacting with Sgr A East, pushing up on it, creating the bend in the southern edge of Sgr A East seen in the color and grey-scale emission in Figures 2 and 4. This region where the SNR is apparently confining Sgr A East is exactly the location of the 1720 MHz OH maser group seen by Yusef-Zadeh et al. (1996) and Yusef-Zadeh et al. (1999). Their data show a group of 8 masers all positioned just inside the southern edge of Sgr A East, along the inward curve caused by the expanding SNR to the south of Sgr A East. Yusef-Zadeh et al. (1999) propose that these masers are due to the expansion of Sgr A East into the 50 km sec^{-1} cloud, as the line of sight velocities of the masers are in the range 53 km sec⁻¹to 66 km sec⁻¹. Our data suggest that the 50 km sec⁻¹cloud lies mainly to the east of Sgr A East and not to the south, as the molecular ridge does not continue along the southern boundary of Sgr A East. However we find plenty of molecular gas in the location of the masers, gas not associated with the 50 km $\rm sec^{-1}cloud$ but rather with the southern streamer as it transports gas from the $20~\rm km~sec^{-1}$ cloud to the nuclear region. The masers appear to lie at the intersection of the SNR as it expands into Sgr A East and the southern streamer as it moves towards the CND. The masers may therefore arise from the expansion of the SNR into the molecular gas in the southern streamer.

The SNR is also interacting with the 20 km \sec^{-1} cloud, creating the sharp linear eastern edge of the GMC seen in the contours of these same figures. The 20 km sec⁻¹cloud does display a backwards "C" shape structure in its position-velocity diagrams (Paper 1, Figure 8) cut b), indicating that this cloud is more behind the SNR than in front of it. The position-velocity diagrams of a cut taken along the lower edge of the cloud in Paper 1 (Figure 8 cut c) show a forward "C" structure, with the gas in the middle of the cut being blueshifted along the line of sight, where presumably the SNR is impacting the 20 km sec⁻¹cloud and disrupting the gas. This interaction may have created the southern streamer. Our velocity dispersion image (Figure 10) shows a pronounced increase in line width in the 20 km sec⁻¹gas located near the "wisp" in the continuum image. The region with the increased line width has an arc morphology, continuing along the bend of the "wisp." This area traces the impact of the expanding SNR on the 20 km sec^{-1} cloud.

This SNR appears to also be interacting with the southern half of the molecular ridge, causing the clear demarcation between the northern and southern halves seen in the kinematics of the gas. The two halves of the ridge have different histories and expanding shells acting on them. The interaction between the SNR and the southern part of the ridge can be seen in the position-velocity diagrams taken along the length of the ridge (see Figure 11). These diagrams not only show large line widths for the emission in the south, but also display a hole in positionvelocity space in the southern half of the diagrams between 35 km sec^{-1} and 70 km sec^{-1} . This may be a shell swept clear by the SNR expanding into the southern part of the streamer. This would place the bulk of the streamer in front of the SNR, and the heated high-velocity emission at $>70~{\rm km~sec^{-1}}$ would be redshifted emission from the streamer that is being pushed away from the observer along the line of sight, on the far side of the SNR. The Ushaped feature in the 1.3mm image (Figure 7) may well be a tilted circular swath of dust from the 20 km sec⁻¹cloud wrapping around the SNR and projected into a U-shape along the line of sight, possibly connecting up with the southern tip of the ridge. The southern part of the ridge may be material from the 20 km sec⁻¹cloud that has been impacted by the expanding SNR, pushing it away from the core of the GMC.

Given the masses of the ridge and the 20 km $\rm sec^{-1}$ cloud, how feasible is it that a SNR could move these features by the 20 km $\rm sec^{-1}$ shift we observe in the position-velocity diagrams? Assuming equipartition of energy in the SNR, roughly half the 10^{51} ergs released in the explosion would be converted to kinetic energy. Using the mass derived in Table 1 for the southern part of the ridge, $0.5 \ 10^{51}$ ergs would be able to displace gas in the

southern ridge by 35 km sec^{-1} . Using the mass derived for the northern part of the 20 km sec^{-1} cloud as reported in Paper 1, a SNR could shift the gas by 15 km sec^{-1} . These numbers are consistent with the observed velocity shifts, so that it is entirely feasible for a typical SNR to cause the observed velocity shifts and increased line widths. The northern part of the ridge shows a 20 km sec^{-1} velocity shift due to the expansion of Sgr A East. Using the derived mass of the northern part of the ridge, we estimate that $4.5 \cdot 10^{50}$ ergs of kinetic energy would be required to cause this movement of the 50 km sec^{-1} cloud, well within the kinetic energy limit of a typical SNR.

It does not appear that the entire molecular ridge was created by the expansion of Sgr A East into the 50 km sec⁻¹cloud, resulting in a narrow shocked region of gas. While the gas in the northern part of the ridge traces the denser parts of the 50 km sec⁻¹cloud, including the western edge of the GMC that Sgr A East is expanding into, the ridge continues to the south past Sgr A East and is being acted upon by other forces in this region. The gas in the southern part of the ridge may have originated in the 20 km sec⁻¹cloud and been pushed to its present position by the expanding SNR. If the narrowness of the ridge in the south is real, in the absence of apparent confinment mechanisms, it could suggest a primordial filamentary structure.

4.3. Line of Sight Locations of Features

With our new data we are able to put constraints on the line-of-sight locations of several of the features at the Galactic Center and begin to build a 3-D model of the region. Figure 13 is a schematic drawing of the large-scale features in the central 15 pc of the Galaxy, with positions shown along the line of sight from the Sun where east is up and west is down. The 20 km sec⁻¹cloud is in front of the nuclear region as seen from the redshift to the north in the velocity gradient along the southern streamer (Paper 1). This places the CND behind the 20 km sec⁻¹cloud, and the 20 km \sec^{-1} cloud in front of the nuclear region. Sgr A East is behind Sgr A West, as Sgr A West is seen in absorption against Sgr A East at 90 cm (Figures 5 and 7 in Pedlar et al. 1989). The 50 km \sec^{-1} cloud is to the east of and slightly behind Sgr A East, as indicated in our position-velocity diagrams where there is redshifted emission from the interaction with Sgr A East but no corresponding blueshifted emission (Figure 11). Along the molecular ridge there is a velocity gradient that redshifts to the north, placing the northern part of the ridge further away from the Sun along the line of sight than the southern part. The SNR to the south of Sgr A East is interacting with the southern part of the molecular ridge which connects to the 50 km sec^{-1} cloud to the north. The SNR is also interacting with the southern edge of Sgr A East, as well as the eastern edge of the 20 km sec^{-1} cloud. The angular size of the SNR is about 3.5', which corresponds to roughly 8.5 pc (at a distance of 8.5 kpc), so that Sgr A East and the 20 km sec⁻¹cloud have to be within 8.5 pc of each other along the line of sight.

4.4. Two Streamers as One Coherent Structure?

The two streamers we image seem to be part of a larger, connected gas cloud complex, as seen from the extended emission in the 1.3mm map and the connections imaged by other groups between the two GMCs in the region. We are missing zero-spacing information in our data, which essentially filters out any structures greater than 1' in size in our maps as well as causes the negative trenches around the strongest emission. In addition, NH₃ only traces the densest gas in the system, so we are not sensitive to less dense gas which may be connecting the streamers. In order to understand the nature of the largescale structure of molecular gas at the Galactic Center, we must compare our maps to the single-dish 1.3mm image (assuming that the dust and gas are well-mixed) and examine surveys of molecular clouds in the region. Güsten, Walmsley, & Pauls (1981) argue that the 20 km sec⁻¹cloud and 50 km sec⁻¹cloud are not only bound to each other but are condensations in a larger complex of 5 gas clouds beginning in the south with the 20 km sec⁻¹cloud and extending almost 2 degrees north of the nucleus. The recent Nobeyama CS J=1-0 survey (Tsuboi, Handa & Ukita 1999) shows a large-scale ridge of gas extending along the Galactic Plane for ≥0.5° at negative latitudes from Sgr A*. The 20 km sec⁻¹cloud and 50 km sec⁻¹cloud appear to be part of this large structure. One obvious question about this structure is why it is offset to negative latitudes and why there is little corresponding emission at positive latitudes.

It is possible that the two streamers we image together make up a tilted ring with respect to our line of sight. A ring-like structure if it were in the plane of the Galaxy would appear as a linear structure from our point of view in the disk, so that morphology alone would not necessarily indicate the presence of a ring; kinematic evidence is needed. Our velocity coverage is limited, sensitive to emission with radial velocities of -35 km sec⁻¹to 100 km sec^{-1} . The Nobeyama survey paper (Tsuboi et al. 1999) presents a position-velocity diagram (their Figure 2b) centered on Sgr A* summed over 16' in latitude which shows half of a ring-type structure in the central 0.5° with emission at positive velocities ranging from 0 km \sec^{-1} to 90 km \sec^{-1} . There is a small region of emission at -20 km sec⁻¹opposing this semi-complete ring which may complete the circle.

5. CONCLUSIONS

A VLA 5-field mosaic of the inner 15 pc of the Galaxy in NH₃(1,1) and NH₃(2,2) emission reveal two long, narrow streamers running roughly along the Galactic plane, each tracing connections between continuum emission in the nucleus and nearby GMCs. The southern streamer is carrying gas from the 20 km sec⁻¹cloud to the CND (see Paper 1). The other streamer, called the molecular ridge, traces the dense parts of the 50 km sec⁻¹cloud, including the core and much of the southern part of the GMC, and wraps around the eastern edge of Sgr A East. The expansion of Sgr A East into the 50 km sec⁻¹cloud is seen as a "C"-shaped structure in position-velocity diagrams of the northern part of the molecular ridge. There is a velocity gradient along the length of the entire streamer

with the gas being redshifted to the north, similar to the gradient seen in the southern streamer connecting the 20 km sec⁻¹cloud to the CND. The molecular ridge closely follows the arc of the Sgr A East continuum emission and continues south past Sgr A East towards the 20 km sec⁻¹cloud. The gas in the southern part of the ridge is perturbed, showing heating and increased line widths, likely the result of an interaction with a SNR south of Sgr A East. This SNR appears to be impacting the 20 km sec⁻¹cloud and Sgr A East as well, placing these features

within 10 pc of each other along the line of sight. Our velocity information allows us to place the 20 km sec⁻¹cloud in front of the CND and Sgr A West, as well as the 50 km sec⁻¹cloud behind Sgr A East. These two streamers appear to be dense peaks of a larger gas complex surrounding the nuclear region.

We would like to thank Cornelia Lang for lending us her VLA 20 cm continuum image and Robert Zylka for sharing his IRAM 1.3mm image.

REFERENCES

Armstrong, J. T. & Barrett, A. H. 1985, ApJS, 57, 535. Coil, A. L. & Ho, P. T. P. 1999, ApJ, 513, 752 (Paper 1). Dent, W. R. F., Matthews, H. E., Wade, R., & Duncan, W. D. 1993, ApJ, 410, 650.

ApJ, 410, 650.

Ekers, R. D., van Gorkom, J. H., Schwarz, U. J., & Goss, W. M. 1983, A&A, 122, 143.

Frail, D. A., Goss, W. M., Reynoso, E. M., Green, A. J., & Otrupcek, R. 1996, AJ, 111, 1651.

Genzel, R., Stacey, G. J., Harris, A. I., Geis, N., Graf, U. U., Poglitsch, A., & Sutzki, J. 1990, ApJ, 356, 160.
Goss, W. M., Schwarz, U. J., van Gorkom, J. H., & Ekers, R. D. 1985, MNRAS, 215, 69.

1985, MNRAS, 215, 69.
Güsten, R., Walmsley, C. M., & Pauls, T. 1981, A&A, 103, 197.
Ho, P.T.P. & Townes, C.H. 1983, ARA&A, 21, 239.
Ho, P. T. P., Jackson, J. M., Barrett, A. H., & Armstrong, J. T. 1985, ApJ, 288, 575.
Ho, P. T. P., Ho, L. C., Szczepanski, J. C., Jackson, J. M., Armstrong, J. T., & Barrett, A. H. 1991, Nature, 350, 309.
Ho, P. T. P. 1994, Astronomy with Millimeter and Submillimeter Wave Interferometry, IAU Colloquium No. 140, Astronomical Society of the Pacific Conference Series, vol. 59, eds. M. Ishiguro and W. J. Welch, p. 161. San Francisco: Astronomical Society of and W. J. Welch, p. 161. San Francisco: Astronomical Society of the Pacific, 1994. 1994amsw.conf..161H

Khokhlov, A. & Melia, F. 1996, ApJ, 457, L61.
Lang, C. C., Morris, M., & Echevarria, L. 1999, ApJ, in press.
Liszt, H. S., van der Hulst, J. M., Burton, W. B., & Ondrechen, M. P. 1983, A&A, 126, 341.
Mezger, P. G., Zylka, R., Salter, C. J., Wink, J. E., Chini, R., Kreysa, E., & Tuffs, R. 1989, A&A, 209, 337.
Pedlar, A., Anantharamaiah, K. R., Ekers, R. D., Goss, W. M., van Gorkom, J. H., Schwarz, U. J., & Zhao, Jun-Hui. 1989, ApJ, 342, 769

Serabyn, E., Lacy, J. H., & Achtermann, J. M. 1992, ApJ, 395, 166. Tsuboi, M., Handa, T. & Ukita, N. 1999, ApJS, 120, 1. Yusef-Zadeh, F., Morris, M., Slee, O. B., & Nelson, G. J. 1986, ApJ,

300, L47.

Yusef-Zadeh, F. & Morris, M. 1987, ApJ, 320, 545. Yusef-Zadeh, F. & Mehringer, D. M. 1995, ApJ, 452, L37. Yusef-Zadeh, F., Roberts, D. A., Goss, W. M., Frail, D. A., & Green, A. J. 1996, ApJ, 466, L25.

Yusef-Zadeh, F., Roberts, D. A., Goss, W. M., Frail, D. A., & Green,

A. J. 1999, ApJ, 512, 230. Zylka, R., Mezger, P. G., & Wink, J. E. 1990, A&A, 234, 133. Zylka, R. 1997, IAUS, 184, 156.

- Fig. 1.— A schematic drawing of the relevant large-scale features in the central 15 pc of the Galaxy showing positions on the plane of the sky with east to the left.
- Fig. 2.— Velocity-integrated maps of NH₃(1,1) and NH₃(2,2) emission in contours from the central 10 by 15 pc of the Galaxy overlaid on a color 20 cm continuum image of Sgr A East and West. Two north-south streamers are seen, one connecting the 20 km \sec^{-1} cloud in the south to the nuclear region, and the other tracing the eastern edge of Sgr A East where it interacts with the 50 km \sec^{-1} cloud and continuing south towards the 20 km \sec^{-1} cloud. The contours levels are -2, -1, 0.1, 1, 2, 3, 4, 5, 6, 7, 8, 9, 10, 11, and 12 Jy beam⁻¹ km \sec^{-1} , integrated over 135 km \sec^{-1} . Five 2' fields have been mosaiced together, and only emission corresponding to a beam response of \ge 15% has been plotted here. The 14.5" by 8.8" beam is shown in the lower left corner of the NH₃(1,1) map. The color continuum image ranges from 0 to .18 Jy beam⁻¹.
- Fig. 3.— The 5-field mosaiced primary beam is seen in dotted contours, with 10% response levels labeled. The NH₃(1,1) velocity-integrated map from Figure 1 is seen in grey-scale and solid contours. NH₃(1,1) emission below a 15% primary beam level has not been shown.
- Fig. 4.— Same as Figure 2 with grey-scale ranging from 0 to .028 Jy beam⁻¹.
- Fig. 5.— Velocity-integrated maps of $NH_3(1,1)$ emission from the southeastern field only on the left and the southwestern field only on the right. No mosaicing was used in these images, so that only data from one pointing is shown in each map. The contours are the same as in Figure 1.
- FIG. 6.— Position-velocity diagrams investigating possible sidelobe contamination in the southern part of the ridge due to the 20 km sec⁻¹cloud. Cut A shows the kinematics along the ridge, while cut B corresponds to the 20 km sec⁻¹cloud. The contours are 0.04, 0.08, 0.12, 0.16, 0.20, 0.24, 0.28, 0.32, 0.36 and 0.40 Jy beam⁻¹ for cut A and 0.1, 0.2, 0.3, 0.4, 0.5, 0.6, 0.7, 0.8, 0.9 and 1.0 Jy beam⁻¹ for cut B.
- Fig. 7.— A 1.3mm continuum image of the central 17.5 by 25 pc of the Galaxy is shown in contours (Zylka 1997), tracing free-free and thermal dust emission. The contour levels are 0.32, 0.47, 0.65, 0.85, 1.20, 1.65, 2.50, and 3.50 Jy beam⁻¹ and the beam size is $\sim 11''$. Our NH₃(1,1) velocity-integrated map is shown in grey-scale from 0 to 8 Jy beam⁻¹ km sec⁻¹.
- Fig. 8.— NH₃(2,2)/NH₃(1,1) velocity-integrated emission is shown in grey-scale with the ratio ranging from 0 to 2. The ratio of NH₃(2,2) to NH₃(1,1) flux reflects heating of the gas, where the dark regions trace heated gas. 20 cm continuum emission from Sgr A East and West is overlaid in contours corresponding to 0.04, 0.06, 0.08, 0.10, 0.12, 0.14, 0.16, 0.18, 0.20 Jy beam⁻¹.
- Fig. 9.— Velocity centroid maps for both the $NH_3(1,1)$ and $NH_3(2,2)$ emission are shown in grey-scale with continuum emission from Sgr A East and West in contours. The grey-scale ranges from 15 km sec⁻¹in white to 60 km sec⁻¹in black, and the 20 cm continuum emission contours are the same as in Figure 8. A velocity gradient is evident along the length of the eastern streamer, where the gas is redshifted in the north where it wraps around Sgr A East.
- Fig. 10.— Velocity dispersion maps for the $NH_3(1,1)$ and $NH_3(2,2)$ data in grey-scale ranging from 0 km sec⁻¹ to 25 km sec⁻¹. The 20 cm continuum emission contours are the same as in Figure 8.
- Fig. 11.— Position velocity diagrams for cuts running north to south along the molecular ridge are shown for the $NH_3(1,1)$ and $NH_3(2,2)$ datacubes, as well as the divided $NH_3(2,2)/NH_3(1,1)$ emission which traces heated gas. The contour levels are 0.04, 0.08, 0.12, 0.16, 0.20, 0.24, 0.28, 0.32, 0.36, 0.40, 0.44, 0.48, 0.52, 0.56 and 0.60 Jy beam⁻¹ for the $NH_3(1,1)$ and $NH_3(2,2)$ diagrams. The $NH_3(2,2)/NH_3(1,1)$ diagrams have a grey-scale ranging from 0 to 2 and the contour levels are 0.5, 1.0, 1.5, and 2.0.
- Fig. 12.— Position velocity diagrams for cuts running east to west across the molecular ridge are shown for the NH₃(1,1), NH₃(2,2) and NH₃(2,2)/NH₃(1,1) datacubes. The contour levels are 0.0250, 0.0625, 0.1000, 0.1375, 0.1750, 0.2125, 0.2500, 0.2875, 0.3250, 0.3625, 0.4000, 0.4375, 0.4750, 0.5125 and 0.5500 Jy beam⁻¹ for the NH₃(1,1) and NH₃(2,2) diagrams. The NH₃(2,2)/NH₃(1,1) diagrams have a grey-scale ranging from 0 to 2 and the contour levels are 0.5, 1.0, 1.5, and 2.0.
- Fig. 13.— A schematic drawing of the large-scale features in the central 15 pc of the Galaxy showing positions along the line of sight from the Sun with east being up.

Table 1 $NH_3(1,1)$ Derived Physical Parameters for the Molecular Ridge

Peak	R.A.; Dec. (B1950)	$ au_m$	$\begin{array}{c} \Delta T_a^* \\ (K) \end{array}$	$T_{ex} \ (K)$	$T_{rot} \ (K)$	$N(J,K) \\ (10^{15} cm^{-2})$	$ N(H_2) (10^{24} cm^{-2}) $	${\rm Mass} \atop (10^5 M_{\odot})$
Northern Southern	17:42:40; -28:59:13 17:42:37; -29:01:23	$\frac{2.0}{1.5}$	4.3 2.8	$7.7 \\ 6.3$	20 30	$5.5 \\ 2.2$	$\frac{1.3}{0.52}$	1.1 0.40

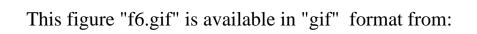
This figure "f1.gif" is available in "gif" format from:

This figure "f2.gif" is available in "gif" format from:

This figure "f3.gif" is available in "gif" format from:

This figure "f4.gif" is available in "gif" format from:

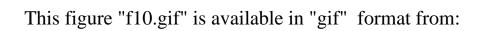
This figure "f5.gif" is available in "gif" format from:



This figure "f7.gif" is available in "gif" format from:

This figure "f8.gif" is available in "gif" format from:

This figure "f9.gif" is available in "gif" format from:



This figure "f11.gif" is available in "gif" format from:

This figure "f12.gif" is available in "gif" format from:

This figure "f13.gif" is available in "gif" format from: